Overview of Multi-Input Frequency Domain Modal Testing Methods with an Emphasis on Sine Testing

Robert W. Rost
David L. Brown

This paper is concerned with an overview of the current state-of-the-art multiple-input, multiple-output modal testing technology. A very brief review of the current time domain methods will be given. A detailed review of frequency and spatial domain methods will be proesented with an emphasis on sine testing.

INTRODUCTION

In the mid sixties sine testing was the only method used for experimental modal analysis. It was used both for the forced normal-mode and the frequency-response methods. With the advent of Fourier Analysis testing methods, sine testing has been used primarily for normal mode testing, for making selected frequency response measurements to study non-linearities; or to gather data in high noise environments.

Sine testing had two major limitations: a) Due to its sweep time, it was considerably slower than the broadband Fourier methods and b) For nonlinear systems, the measurements were distorted. The distortion caused problems with the parameter estimation methods, however, it should be noted that the distortion is important for characterizing non-linearities. The practical advantage of sine testing included high signal-to-noise-ratio and controllable spectrum content.

Unfortunately this method was only competitive with random excitation when large numbers of transducers were permanently mounted to the test structure. In the past, considerable investment in transducer instrumentation limited sine testing to laboratories with significant resources.

As a result, in the early seventies single input random excitation became the method of choice for laboratory modal testing. In the late seventies, multiple-input random excitations methods were developed to generate a consistent database to work with the multiple-input parameter estimation algorithms under development at that time. These algorithms were primarily time domain algorithms which fit the measured multiple-input unit impulse or initial conditions responses. In order, to generate a consistent database, it is necessary to measure all of the response data simultaneous which again creates the situation which existed with sine testing. That is the requirement to monitor many transducer channels at once.

Recently, low cost instrumentation introduced by PCB Piezotronics[1-4], makes multiple-input/ multiple-output frequency response function analysis affordable for the smaller testing laboratories with less resources. The continuing decrease in the per channel cost of measurement systems encourages multiple channel testing for experimental modal analysis. With this inexpensive multi-channel instrumentation, stepped sine excitation competes favorably with random excitation. That is, more test laboratories can now afford the many transducers required to make stepped sine test competitive.

As shown in Fig. 1, at higher numbers of channels sine testing is more efficient than broadband testing. This advantage is due to the fact that as the number of channels increases, the signal processing overhead increases more rapidly with random testing because sine testing is limited by sweep time instead of signal processing.

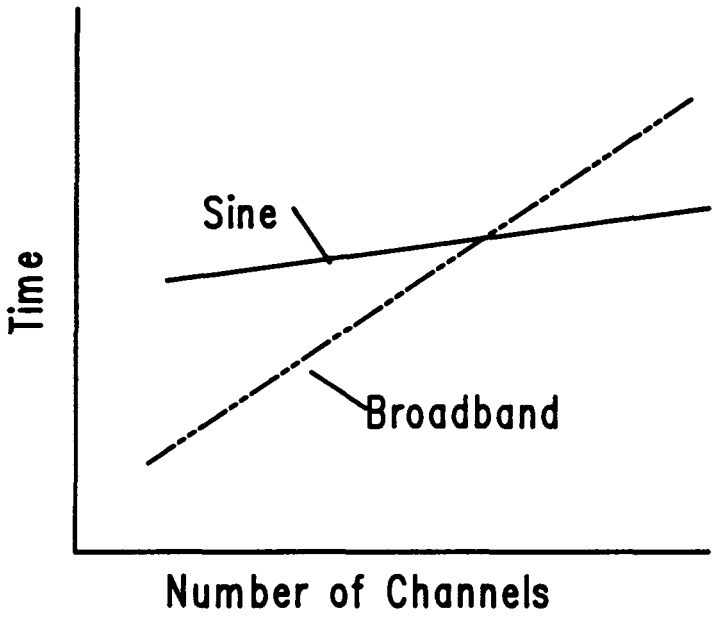

Figure 1. Comparison of sine vs. broadband testing

In fact for a test with six references and 750 response measurements, in the near future, a simple desktop computer will be able to perform the necessary signal processing. In contrast, for the same number of input and output points random testing would require a very powerful computer to perform real-time-signal processing.

To improve sine testing the new system being developed at UCSDRL implements a novel testing ideal called "spatial sine testing" (SST). Unlike the frequency response methods (FRF) which develops a data base of frequency response functions(temporal information) the new SST method develops a data base of forced modes of vibration(spatial information). This SST method also differs from the normal-mode method, which measures directly only the normal modes by a force appropriation technique.

The testing procedure in the SST method excites the structure with a forcing vector at preselected but arbitrary frequencies and measures the forced complex mode of vibration with an array of transducers. It stores this complex forced mode of vibration into the database along with the frequency and the measured forcing vector. The forcing vector and the frequency are chosen to generate a database of temporal and spatial information: not to tune a mode as in the normal-mode method. At a given frequency, the SST measures multiple forcing vectors and the resulting forced modes of vibration, and stores the results in the database.

Currently several advanced multiple reference parameter identification algorithms are capable of processing data from this kind of modal test. These methods process the data both in the frequency

and the spatial domain.

SPATIAL DOMAIN

In the area of parameter identification, the spatial domain is a relatively new thought process . This concept describes the system frequency and/or impulse response function matrix in terms of the complex dot product of three fundamental characteristic functions; two complex spatial, and one complex temporal. The spatial characteristics are a function of geometry and the temporal characteristics a function of either time or frequency.

Thus, the measured frequency response function matrix can be described in this three dimensional complex space as functions of three sampled characteristic variables (p,q,ω_k). In other words, the frequency response functions occurred at discrete reference points q, response points p, and discrete frequencies ω_k.

This concept is difficult to visualize, since the matrix is represented by three dimensional complex characteristic space (Fig. 2). To more easily understand the process, view the variation along lines parallel to axes of the space. Lines parallel to the temporal axis correspond to individual frequency response functions (or unit impulse response functions in time domain). These frequency response functions consist of a summation of the temporal characteristics (unit amplitude SDOF frequency response functions), weighted by the two spatial characteristics, which define the other two axis of the characteristic space.

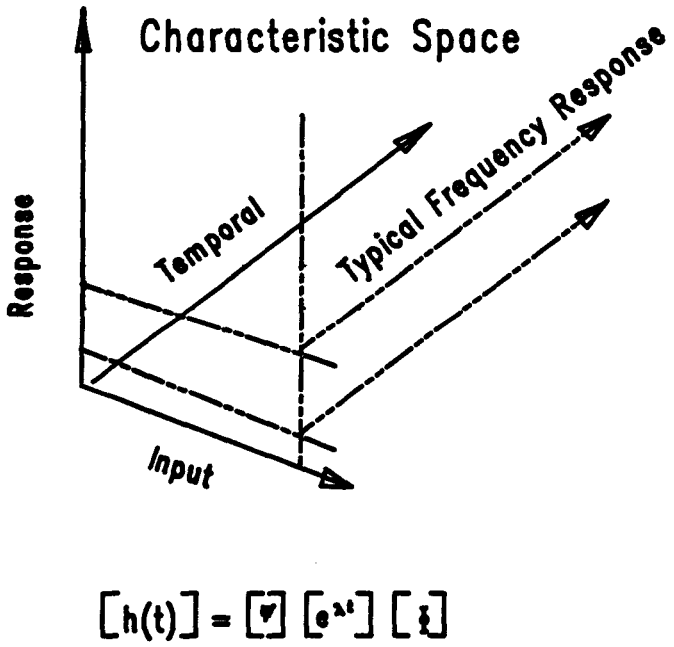

Figure 2. Spatial domain

Lines parallel to the response axis correspond to forced modes of vibration. These forced modes consist of a summation of the system eigenvectors weighted by the input characteristic and the

temporal characteristic.

Likewise, lines parallel to the input, or reference axis consist of a summation of the system eigenvectors weighted by the response characteristic and the temporal characteristic. The variation along these lines are referred to in the literature as the modal participation factors.

THEORY

In this section a brief summary of the algorithms that are currently being studied for use with the SST method will be given. These algorithms are the Polyreference Frequency Domain[5,6], the Multiple Reference Orthogonal Polynomial[7-9] and the Multi-MAC method[10-11]. Multi-MAC is a technique that seems well suited for the spatial domain sine test data. It is a spatial domain technique that temporally weights the forced modes of vibrations in determining the modal characteristics the test article.

POLYREFERENCE FREQUENCY DOMAIN

The displacement frequency response function for multiple input/output is given by:

$$[H_d(s)]_{N_0 \times N_i} = [\Psi][s\,\Gamma I_\rfloor - \Gamma \Lambda_\rfloor]^{-1}[L] \tag{1}$$

where:

- s Laplace variable
- $[H_d(s)]$ the transfer function matrix of size $N_0 \times N_i$, which is the Laplace transform of the impulse response matrix $[h(t)]$
- $[\, s\,\Gamma I_\rfloor - \Gamma \Lambda_\rfloor \,]^{-1}$ Laplace transform of $e^{\Gamma \Lambda_\rfloor t}$
- $\Gamma I_\rfloor$ identity matrix

The subscript d on the $[H]$ matrix indicates that the transfer function matrix is in terms of displacement over force. In order to obtain an expression for the transfer function in terms of velocity and acceleration in the frequency domain, the Laplace transformation properties can be applied immediately to Eq. (2). The resulting two equations, obtained for the transfer function matrix with respect to the velocity and the acceleration, are:

$$[H_v(s)]_{N_0 \times N_i} = s[H_d(s)] - [h(t)_{t=0}] \tag{2}$$

$$= s[H_d(s)] - [\Psi][L] \tag{3}$$

and

$$[H_a(s)]_{N_0 \times N_i} = s^2[H_d(s)] - s[h(t)_{t=0}] - [\dot{h}(t)_{t=0}] \tag{4}$$

$$= s^2[H_d(s)] - s[\Psi][L] - [\Psi]\,\Gamma \Lambda_\rfloor\,[L] \tag{5}$$

In order to compensate for the influence of the modes outside the frequency range of interest, an additional term can be added to the previous equations to compensate for these residuals effects. Adding the residual terms to Eq. (1), (3) and (5) and simplifying Eq. (3) and (5), by substituting the matrix $[T]$, the equations become :

$$[H_d(s)] = [\Psi]\,[T(s)] + [R_d] \tag{6}$$

$$[H_v(s)] = [\Psi]\,\lceil\Lambda\rfloor\,[T(s)] + [R_v] \tag{7}$$

$$[H_a(s)] = [\Psi]\,\lceil\Lambda\rfloor^2\,[T(s)] + [R_a] \tag{8}$$

where

- $[T(s)] = [s\,\lceil I\rfloor - \lceil\Lambda\rfloor]^{-1}$ is a matrix of size $2N \times N_i$
- $[R_d]$ matrix for the residual effects of displacement, of size $N_0 \times N_i$
- $[R_v]$ matrix for the residual effects of velocity, of size $N_0 \times N_i$
- $[R_a]$ matrix for the residual effects of acceleration, of size $N_0 \times N_i$

Equations (6), (7) and (8) can be combined into one equation:

$$\begin{bmatrix}[H_d(s)]\\ [H_v(s)]\\ [H_a(s)]\end{bmatrix}_{3N_0\times N_i} = \begin{bmatrix}[\Psi]\\ [\Psi]\,\lceil\Lambda\rfloor\\ [\Psi]\,\lceil\Lambda\rfloor^2\end{bmatrix}_{3N_0\times 2N} [T(s)] + \begin{bmatrix}[R_d]\\ [R_v]\\ [R_d]\end{bmatrix}_{3N_0\times N_i} \tag{9}$$

It can be shown [13]that the characteristic equation, associated with Eq. (9) is of the form :

$$\left[\,[A_0]^T\;[A_1]^T\;\lceil I\rfloor\,\right]_{N_0\times 3N_0} \begin{bmatrix}[\Psi]\\ [\Psi]\,\lceil\Lambda\rfloor\\ [\Psi]\,\lceil\Lambda\rfloor^2\end{bmatrix}_{3N_0\times 2N} = [0]_{N_0\times 2N} \tag{10}$$

Equation (10) represents a matrix polynomial of order 2. Since the matrix coefficients have a dimension of N_0 this matrix polynomial has $2N_0$ poles. The 2N system poles represented by the matrix $\lceil\Lambda\rfloor$ are a subset of these $2N_0$ poles. The unknown matrix coefficients of the matrix polynomial, can be obtained from next equation [13]:

$$\left[\,[A_0]^T\;[A_1]^T\;\lceil I\rfloor\,\right] \times \begin{bmatrix}[H_d(s)] - [R_d]\\ s\,[H_d(s)] - [\Psi][L] - [R_v]\\ s^2\,[H_d(s)] - s\,[\Psi][L] - [\Psi]\lceil\Lambda\rfloor[L] - [R_a]\end{bmatrix} = [0] \tag{11}$$

This equation means that the measured FRF's can be described by a linear frequency domain model with real matrix coefficients:

$$[A_0]^T\,[H_d(s)] + s\,[A_1]^T\,[H_d(s)] + s^2\,[H_d(s)] = s\,[R_1] + [R_0] \tag{12}$$

where:

- $[R_1] = [\Psi]\,[L]$ and is equal to the residue matrix.
- $[R_0] = \left[[A_1]^T\,[\Psi] + [\Psi]\,[\Lambda]\right][L] + [A_0]^T[R_d] + [A_1]^T\,[R_v] + [R_a]$

The unknown matrices $[A_0]$, $[A_1]$, $[R_1]$ and $[R_0]$ are calculated by solving Eq. (12) in a least squares sense. The solution of the generalized eigenvalue problem, defined by Eq. (11), directly yields the complex system poles and the corresponding mode shapes for the structure.

MULTIPLE-REFERENCE ORTHOGONAL POLYNOMIAL METHOD

For a N degree-of-freedom linear system with viscous damping, the multiple-reference orthogonal polynomial method yields an auto-regressive moving average (ARMA) model of order (m,n) :

$$\sum_{k=0}^{m} [a_k]\, s^k \quad [H(s)] = \sum_{k=0}^{n} [b_k]\, s^k \tag{13}$$

where:

- $[H(s)]$ *transfer function matrix* of size $N_o \times N_i$.
- $[a_k]$ matrix polynomial coefficient of size $N_o \times N_o$.
- $[b_k]$ matrix polynomial coefficient of size $N_o \times N_i$.
- m order of matrix polynomial chosen in the Auto-Regressive part. $mN_o \geq 2N$.
- n order of matrix polynomial chosen in the Moving-Average part. $n \geq m+2$.
- N the degree-of-freedom of the system or the number of modes
- N_i number of excitation location.
- N_o number of response point.

In order to avoid the numerical ill-conditioning in Eq.(13), a set of complex orthogonal polynomials, with weighting function $q(s)$, is defined as:

$$\sum_{i=1}^{l} p_j(s_i)\, q(s_i)\, p_k(s_i)^* = \delta_{jk} \tag{14}$$

For the specific frequency range, these polynomials need be generated only once. The ARMA modal can then be expressed in this orthogonal basis, in which the numerical ill-conditioning can be avoided. The ARMA model is expressed as:

$$\sum_{k=0}^{m} [\alpha_k]\, p_k \quad [H(s)] = \sum_{k=0}^{n} [\beta_k]\, p_k \tag{15}$$

where:

- $[\alpha_k]$ matrix polynomial coefficient for orthogonal polynomials of size $N_o \times N_o$.
- $[\beta_k]$ matrix polynomial coefficient for orthogonal polynomials of size $N_o \times N_i$.
- p_k orthogonal polynomial of order k, which is a scalar function.

By choosing $[\alpha_m] = \lceil I \rfloor$, Eq.(15) can be arranged and rewritten in matrix form for all spectral lines.

$$\begin{bmatrix} [H]^H[P_0]^H & \cdots & [H]^H[P_{m-1}]^H & -[P_0']^H & \cdots & -[P_n']^H \\ & & \vdots & & & \\ & & & & & \\ & & & & & \\ & & & & & \\ & & & & & \\ & & & & & \\ & & & & & \\ & & (\text{for } s = j\omega_i ,\ i=1,2,\ldots, l \text{ spectral line}) & & & \end{bmatrix}$$

$$\times \begin{bmatrix} [\alpha_0]^T \\ [\alpha_1]^T \\ \vdots \\ [\alpha_{m-1}]^T \\ [\beta_0]^T \\ [\beta_1]^T \\ \vdots \\ [\beta_n]^T \end{bmatrix} = \begin{bmatrix} -[H]^H[P_m]^H \\ \cdot \\ \cdot \\ \cdot \\ \cdot \\ \cdot \\ \cdot \\ \cdot \end{bmatrix} \tag{16}$$

where:

- $[P_k]^H$ product of p_k^* and identity matrix $\lceil I \rfloor$ of size $N_o \times N_o$.
- $[P_k']^H$ product of p_k^* and identity matrix $\lceil I \rfloor$ of size $N_i \times N_i$.

The matrix coefficients in Eq.(16) can then be found by formulating the normal equation and solving the simultaneous equation. A transformation matrix is calculated in the polynomial generating procedure; thus, the power polynomial coefficients $[a_k]$ and $[b_k]$ can be calculated from orthogonal polynomial coefficients $[\alpha_k]$ and $[\beta_k]$ respectively. Once the $[a_k]$'s are found, the poles of the system, natural frequencies and damping characteristics, can be solved by setting the determinant of the characteristic equation equal to zero.

$$\det\left(\sum_{k=0}^{m} [a_k]\, s^k \right) = 0 \tag{17}$$

There are two ways of finding the residue matrices. One is to directly use the power polynomial coefficients $[a_k]$ and $[b_k]$

$$[A_r] = \lim_{s \to \lambda_r} (s - \lambda_r)\, [a(s)]^{-1}\, [b(s)] \tag{18}$$

where:

- $[a(s)] = \sum_{k=0}^{m} [a_k]\, s^k$
- $[b(s)] = \sum_{k=0}^{n} [b_k]\, s^k$

Since $[a(s)]$ is singular as $s \to \lambda_r$, the singular value decomposition is used for finding the generalized inverse of $[a(s)]$, then the residue matrices calculated. Another way of calculating residue matrices is in a second stage residue calculation. Base upon the pole information (frequency and damping) and the modal participation factors, obtained in solving the companion matrix of Eq.(17), a least square residue calculation for multiple reference FRF is applicable.

MULTI-MAC ENHANCED FRF METHOD

Multi-Mac is an extension of the concept of Modal Assurance Criterion (MAC). The concept of MAC is a calculation that is used to gain confidence in the estimates of modal vectors either by verifying that the estimates of different modal vectors are unique, that normal modes have been estimated, or that estimates from different rows or columns of the residue matrix for the same mode are identical. Multi-Mac is a spatial domain method of determining modal parameters based on multiple-reference frequency response functions. For linear systems with normal modes, the residue of any input/output combination is made up of three parts, the modal vector at the input location, the modal vector at the output location, and the scaling constant for that mode[10,11,19].

$$A_{pqr} = Q_r \psi_{pr} \psi_{qr} \tag{19}$$

Equation 19 can be expanded to form the complete residue matrix for any mode r.

$$[A_r] = Q_r \begin{bmatrix} \psi_{1r}\psi_{1r} & \psi_{1r}\psi_{2r} & \psi_{1r}\psi_{3r} & \cdots \\ \psi_{2r}\psi_{1r} & \psi_{2r}\psi_{2r} & \psi_{2r}\psi_{3r} & \cdots \\ & & & \\ \psi_{mr}\psi_{1r} & \psi_{mr}\psi_{2r} & \psi_{mr}\psi_{3r} & \cdots \end{bmatrix} \tag{20}$$

Where:

- A_{pqr} Residue for mode r at response point p and reference point q.
- $[A_r]$ residue matrix for mode r of size $N_o \times N_i$
- Q_r Scaling constant for mode r
- ψ_{pr} Modal vector for location p of mode r
- ψ_{qr} Modal vector for location q of mode r

From Eq.(20) it can be seen that there must be a linear relationship between any row or any column of the residue matrix for a particular mode. For example, if the structure was excited at points 1 and 2, then in column one every residue would have ψ_{1r} in common. Likewise, every residue in column two would have ψ_{2r} in common. The modal vectors at the output locations, ψ_{1r} through ψ_{mr}, must therefore be related since they define the same mode. If this linear relationship does not exist, either measurement errors have contaminated the data, the modes are closely coupled or, there is a repeated root at that pole location so that the residue is a linear combination based on input location. Also, from the basic theory of modal analysis, the modal vectors of two different modes must be orthogonal with each other and a weighting matrix such as the mass matrix. If estimates of the residues for the same mode but for different rows or columns is used, a principal component analysis can be used to determine the number of independent vectors that make up those residues. If one significant eigenvalue is found from the principal component analysis, then one mode is presented. If more than one significant eigenvalue is calculated, then there are more than one set of independent vectors that make up the residue matrix for that mode. Eq.(20) can be used to set up the principal component analysis. The size of the matrices is determined by the number of measurement locations and the number of modal vector estimates. The residue matrix can have more than one estimate of the modal vector for the same input/output locations. These estimates could be from different curve fitting algorithms.

$$[\overline{A_r}]^H [\overline{A_r}] = [W] [V] \lceil \Sigma \rfloor [V]^T [W]^T \tag{21}$$

Where:

- $[\overline{A_r}]$ estimated residue matrix of size $N_o \times N_k$, which is generated by putting N_k estimated modal vectors together side by side.
- $[W]$ diagonal weighting matrix of size $N_k \times N_k$
- $[V] = [v_1\ v_2\ \cdots\ v_{N_k}]$ is the matrix of eigenvectors
- $\lceil \Sigma \rfloor$ is the diagonal eigenvalue matrix

Eq.(21) will yield as many eigenvalues as the number of rows in the residue matrix. Some of these eigenvalues will be zero or of insignificant value. The number of significant eigenvalues will indicate the number of independent vectors that make up the residues at that frequency. Associated with each eigenvalue will be the eigenvectors for that eigenvalue which will number as many as the number of rows in the residue matrix. The weighting matrix that was used in Eq.(21) for this work was the identity matrix. A better weighting matrix would be to use the inverse of the square root of the mass matrix or an estimate of the inverse of the square root of the mass matrix from a finite element analysis. The matrix could also be an error matrix or a matrix that would allow different types of data in the residue matrix. For example, if both acceleration and displacement data was contained in the residue matrix, the multiplication of acceleration and displacement would not be dimensionally correct. But, the weighting matrix could be used to make the multiplication dimensionally correct[10]. Any estimate of the residue may be used in this procedure. Since, at resonance, the quadrature part of the frequency response function is proportional to the residue, the simplest method is to use the peak of the imaginary part of the frequency response estimate as an estimate of the residue. If leakage is present in the data, it is advantageous to use spectral lines that are adjacent to the highest peak in the imaginary part. These spectral lines will be less contaminated by leakage. In experimental procedures, the principal component analysis is applied for the quadrature part of FRF matrix, either one or several adjacent spectral lines are included in the analysis each time. This will yield a set of eigenvalues, which equals to the number of adjacent spectral lines by the number of references, for each analysis. The analysis can be exercised over the whole spectral range. All of these eigenvalues can then be plotted as a function of frequency, namely Complex Mode Indicator Function (CMIF)[5]. in which the significant eigenvalue peaks indicate normal modes nearby and the corresponding eigenvectors will be the independent vectors that make up the residue vectors at that frequency. Once the eigenvalues and eigenvectors have been calculated by the principal component analysis, the residues can be transformed to a new coordinate space which are mathematically guaranteed to be orthogonal with each other and the assumed weighting matrix. Therefore, if more than one eigenvalue of significant value is found, the orthogonal mode shapes that make up the estimate of the residue at that frequency can be computed. For example, if there are repeated roots, the residues that make up that repeated root will be calculated. If the modes are heavily coupled, unique modes will be estimated. But, the transformed modes will have the contamination of other modes removed and will be orthogonal with each other. Eq.(22) defines the transformation from the original residues to the new space for i'th significant eigenvalue. This transformation would be used for each eigenvalue of significant value. Therefore, if more than one eigenvalue of significant value is found, the transformation will yield orthogonal estimates of the residues. If more than one estimate of the residue is used for each row or column, these transformed estimates are summed together to reduce the variance. The matrix multiplication will therefore yield one residue for each measurement location. The variance of the modal vectors will be reduced in a least squares sense by $[1/n]^{1/2}$, where n is the number of average.

$$\{A_r\}_i' = [\overline{A_r}]\{v_i\} \tag{22}$$

The residue vectors can then be transformed by these eigenvectors. These transformed residues could be weighted by the mass matrix to yield mode shapes of the system. These new mode shapes are mathematically guaranteed to be orthogonal with each other. Using these transformed estimates of the residue vectors, an enhanced frequency response function can be computed which can be fit for estimates of the frequency and damping of that mode.

Note that the mode shapes found here were arbitrary scaled. The correct scaling can be made, after the frequency and damping values were found, by other residue calculation algorithms, ie. least square frequency residue calculation algorithm.

ANALYTICAL CASES

To compare the spatial domain characteristics of the Polyreference Frequency Domain (PFD), Multiple-Reference Orthogonal Polynomial (MROP) and the Multi-Mac Enhanced FRF (MMEFRF) algorithms, a theoretical data set of 9 references (3 point, 3 direction) and 270 responses (90 point, 3 direction) was generated. This data set was generated by synthesizing the modal parameters (frequency, damping and mode shape) of the "H-frame". The "H-frame" is a steel structure made for testing purposes at the University of Cincinnati Structural Dynamics Research Lab (UCSDRL). The geometry of the structure is shown in Figure1, with the reference point numbers circled. The modal model of the "H-frame" contains 19 modes. The modal frequencies and damping values are listed in Table 1, and the original mode shapes are shown in Figure 2. Since this data set is generated from the modal parameters of the actual structure, there is no significant physical loss. Since the exact modal parameters are known, the accuracy of these algorithms can be evaluated. The algorithms currently implemented at the UCSDRL are limited to six references. Therefore, the data was analyzed with six references taken from the set of nine. Two cases with different reference selections were studied.

The six references used in the first data set correspond to the three coordinate directions at points 72 and 75. As can be seen from Figure 1, any local mode of the cross beam will be poorly excited from these locations. For example, the mode at 312.6 Hz is a local mode of the cross-beam. Therefore, some difficulties might be expected with the estimation for this particular pole.

Figure 3 shows a typical driving point frequency response function for this data set. All three frequency domain algorithms were used to analyze this data set. For the PFD and the MROP, the analysis was done over several frequency bandwidth. This is normal since frequency domain algorithms are not suitable, in general, for large frequency ranges due to numerical problems. On the other hand, the MMEFRF was used over the complete frequency range. This method does not have the same numerical problems as the other two methods.

The complex mode indicator function (CMIF) is a plot of the eigenvalues of a principal component analysis with the redundent residue information as the input to the algorithm. If only one mode shape exists at a given frequency, the principal component analysis will have one eigenvalue of significant values with all other eigenvalues of insignificant value. The number of eigenvalues calculated depends on the size of the analysis. If a natural frequency is a repeated pole, the principal component analysis will have two significant eingenvalues for that frequency. Also, if the pole is a closely spaced root, the principal component analysis will yield as many eigenvalues as independent modes active at that frequency.

The MROP and MMEFRF both use the complex mode indicator function [5] (CMIF) to determine the number of modes in the frequency range of interest. The CMIF plot for the first data set is shown in Figure 4. The way to read a CMIF plot is as follows. The plot of the largest eigenvalue peaks wherever there is a pole. If a repeated pole exists, the plot of the second largest eigenvalue will peak at the same frequency as the plot of the largest eigenvalue. From Figure 4, it can be seen that the plot of the largest eigenvalue peaks at 18 different places, which means that the algorithm finds 18 poles in the whole frequency range. However, the data set was generated using 19 poles. Taking a closer look in the 312 Hz frequency range, the plot of the second largest eigenvalue peaks in this frequency range. Normally, the plot of the second largest eigenvalue peaks between poles. This means that the forced mode of vibration is a linear combination of two independent modes. While at a resonance frequency the plot of the second largest eigenvalue is very small, which means that only one mode is

contributing to the forced mode of vibration. However, for this frequency the second pole is separated from the previous one to explain this peak. In this case, the CMIF plot indicates that there is a mode at this particular frequency. But this mode is not well excited from the references that were chosen. For this data set it was possible to find this pole by overdetermining the order of the polynomial in the case of MROP or by requiring the vector associated with the second largest eigenvalue at that frequency for the MMEFRF case. In the case of the PFD, the algorithm found this frequency but flagged it as a computational pole. So all three algorithms had some problems in detecting the particular mode that was poorly excited from the chosen references.

In the case of MMEFRF, the mode shapes are calculated in the first step. If the frequency and damping of the poles are required, an enhanced frequency response function is calculated for each pole. Then, this enhanced frequency response function is used to estimate the frequency and damping values using only the single reference algorithms. Since the enhanced FRF may be contaminated by other modes, it is necessary to use multiple modes algorithms for good frequency and damping estimations. For this example the single reference orthogonal polynomial method, which is a special case of MROP, is used for the frequency and damping estimation. If the frequency spacing of the enhanced FRF is evenly spaced, time domain algorithms such as Least Square Complex Exponential can also be used. The estimated frequency and damping values for each mode and each method can be found in Table 1. As can be seen from this Table, the MROP and MMEFRF are estimating the poles very well. The PFD gives a good estimate of the pole values but they are not as accurate at the ones obtained with the two other methods.

As a check on the accuracy of the estimated modes, a modal assurance criterion was calculated between the estimated modes for each of the algorithms, and the original mode shapes that were used to create the data set. The results can be found in Table 2. From these results, it can be concluded that all three methods found the correct mode shapes, except for the MMEFRF method, which had a poor estimate of 14th mode shape.

The modal parameters were estimated again on a second data set, using the MMEFRF method. This data set included the reference point 15 in the X direction, which replaced reference 75 in the Z direction. It was used to demonstate a set in which the 14th mode is well excited. If the interpretation of the CMIF plot, for the first data set, was correct, a CMIF plot should now be obtained in which the 14th mode shows up in the the plot of the largest eigenvalue. The second reason was to see if the MMEFRF could find a better estimate for the mode shape of the 14th pole, when this mode is well excited. The CMIF plot, that was obtained for this data set, is shown in Figure 5. As was expected, the 14th mode, which was better excited in this data set, shows up in the plot of the largest eigenvalue. The modal parameters that were found for this particular pole with MMEFRF improved and can be found in the last column of Tables 1 and 2.

As can be seen in Tables 1 and 2 all three methods gives good results on theoretical data as expected. With the PFD amd MROP methods it was necessary to break the frequency range into bands and estimate the number of modes in each band. The MMEFRF method could use the complete band and the number of modes and the modal coefficients were estimate directly from the CMIF. The MMEFRF method is simpler and faster to use but does not handle closely coupled modes as well as the other two methods at least for ideal data.

Some preliminary studies have been preformed with various types of noise added to the measurements. These results are sketchy and will be repeated in the future so that all the methods experience equivalent testing conditions. The test which have been performed indicates that all the methods handles random noise well but perform poorly with data which has frequency shifts. This was expected since it has been a consistent observation with all of the multi-input parameter estimation methods(time and frequency). It should be noted that it is the frequency shift problem with the multi-input algorithms which has led to testing procedures where all of the response data is measured simultaneous.

SYSTEM CONCEPT

As mentioned in the introduction the UCSDRL has been developing a spatial domain sine testing system (SST) with practicality, simplicity and low cost as goals. This system will help the experimentalist obtain a consistent, valid database. The system being developed attempts to minimize test setup time allowing more time for data acquisition and analysis. By instrumenting large numbers of data points (typically 64, 128, etc.), the lightweight motion sensors provide a more comprehensive data base while adding only a minimal, constant mass distribution. Accordingly, the resultant data base displays better spatial definition without the frequency shifts inherent in the method of "roving" accelerometers.

Modular mounting, wiring and calibration equipment eliminate many of the historic problems with setup, identification, calibration and management of large numbers of channels of data. Sensor signals are routed to patch panels which consolidate the individual cables into multiconductor ribbon cables carrying signals on to the signal conditioning equipment. Managing all channels in parallel, the signal conditioning automatically sets maximum gain and anti-aliasing filters the signals. Inexpensive digitizing and signal processing follow as the final steps in the data acquisition.

The force appropriation equipment consists of shakers, amplifiers and a low cost computer-controlled multiple channel digital to analog converter (DAC) system. The multiple channel DAC system currently under development would typically consist of 4, 8, or more channels (up to 32 channels) individually controlled from the system controller. The signal from each channel would be independently set for magnitude and phase. Several prototypes have been built and are currently being evaluated.

A personal computer controls the system, including the signal processing functions. Ideally, the personal computer should be able to acquire the data in real time. Although processing up to 512 channels of data seems like an insurmountable task for a personal computer, a four point discrete Fourier transform(DFT) considerably reduces the volume of data being processed. Since the signal conditioning contains anti-aliasing filters the sinusoidal signals do not need to be oversampled to gain the desired amplitude accuracy. Instead a simple four point DFT, involving only two additions, can be performed on the sinusoidal signals significantly reducing the amount of information processing overhead. In other words, for a 512 channel sine test only 2048 pieces of information need to be processed and stored in computer memory at one time and transformed into the frequency domain with 1024 additions. With an additional eight additions per channel, adaptive processing can be implemented to determine the signal-to-noise-ratio. As a result, the system could adaptively determine the number of averages needed to produce acceptable data at each frequency.

SUMMARY

The advent of current low cost per channel instrumentation creates a competitive forum for broadband modal testing. Now large data acquisition systems can be assembled less expensively than ever before. This economy stimulates renewed interest in sine testing, as the situation now exists where large scale sine testing systems can compete economically with broadband testing systems. Such a large scale spatial domain sine testing system is presently under development at UCSDRL.

Conceptually, the spatial domain sine testing system typically consists of up to 512 or more channels of STRUCTCEL motion sensors linked by the data acquisition system (DATA HARVESTER) with a personal or a small technical computer. The computer processes the data, archives the results and generates the excitation signal with a multiple channel DAC. A simple four point DFT significantly reduces the computational overhead of processing large channels of data. The spatial domain sine testing system essentially integrates available low cost instrumentation with sine excitation and

advanced spatial and frequency domain parameter identification. The purpose of this research is to determine if spatial sine testing will become one of the next generations of modal testing methodologies.

ACKNOWLEDGEMENTS

The work described in this paper was partially supported by the U.S. Air Force under the contract "Experimental Modal Analysis and Dynamic Component Synthesis", Contract No. F-33615-83-C-3218.

The authors would also like to thank Tony Severyn, Filip Deblauwe, and C. Shih of the UCSDRL for their contribution to this paper.

REFERENCES

[1] Brown, D. L., "Keynote Speech - Modal Analysis - Past, Present and Future", Proceedings of the First International Modal Analysis Conference, Orlando Florida, November 1982.

[2] Lally, R. W., Poland, J. B., "A Low Cost Transducer System for Modal Analysis and Structural Testing", Sound and Vibration, January 1986.

[3] Poland, J. B., "An Evaluation of a Low Cost Accelerometer Array System, Advantages and Disadvantages", Master of Science Thesis, University of Cincinnati, Dept. of Mechanical and Industrial Engineering., 1986.

[4] Lally, M. J., Brown, D. L., "STRUCTCEL- A New Instrumentation System", Fourteenth Transducer Workshop, Colorado Springs Colorado, June 1987.

[5] Zhang, L., Kanda, H., Brown, D. L., Allemang, R. J., "A Polyreference Frequency Domain Method for Modal Parameter Identification", ASME Paper Number 85-DET-106, 1985.

[6] Lembregts, F., Snoeys, R. and Leuridan, J., "Multiple Input Modal Analysis of Frequency Response Functions Based on Direct Parameter Identification", Tenth International Seminar on Modal Analysis Part IV, University of Leuven Belgium, 1985.

[7] Shih, C. Y., Tsuei, Y. G., Allemang, R. J., Brown, D. L., "Extension of a Parameter Estimation Method to Multiple Reference Frequency Response Measurements", Eleventh International Seminar on Modal Analysis, University of Leuven Belgium, 1986.

[8] Vold, H., "Orthogonal Polynomials in the Polyreference Method", Eleventh International Seminar on Modal Analysis, University of Leuven Belgium, 1986.

[9] Van Der Auweraer, H., Leuridan, J. L., "Multiple Input Orthogonal Polynomial Parameter Estimation", Eleventh International Seminar on Modal Analysis, University of Leuven Belgium, 1986.

[10] Rost, R. W., "Investigation of Multiple Input Frequency Response Function Estimation Techniques for Modal Analysis", Doctor of Philosophy Dissertation, University of Cincinnati,1986.

[11] Allemang, R. J. "Investigation of Some Multiple Input/Output Frequency Response Function Experimental Modal Analysis Techniques" Doctor of Philosophy Dissertation University of Cincinnati Mechanical Engineering Department 1980, 358 pp.

[12] Allemang, R.J., Rost, R.W., Brown, D.L., "Multiple Input Estimation of Frequency Response Function: Excitation Considerations", ASME Paper Number 83-DET-73.

[13] Leuridan, J. "Some Direct Parameter Model Identification Methods Applicable for Multiple Input Modal Analysis" Doctoral Dissertation Department of Mechanical Engineering University of Cincinnati 1984, 384 pp.

[14] Vold, H., "Orthogonal Polynomials in the Polyreference Method", Proceedings, Eleventh International Seminar on Modal Analysis, Belgium, 1986.

[15] Van Der Auweraer, H., Leuridan, J.M., "Multiple Input Orthogonal Polynomial Parameter Estimation", Proceedings, Eleventh International Seminar on Modal Analysis, Belgium, 1986.

[16] Williams, R., Crowley, J., Vold, H., "The Multivariate Mode Indicator Function in Modal Analysis", 3rd IMAC, 1985.

[17] Brown, D.L., Zimmerman, R.D., Allemang, R.J., Mergeay, M., "Parameter Estimation Techniques for Modal Analysis", SAE Paper Number 790221, SAE Transactions, Volume 88, pp. 828-846, 1979.

[18] Allemang, R.J., Brown, D.L., Rost, R.R. "Multiple Input Estimation of Frequency Response Functions for Experimental Modal Analysis" U.S. Air Force Report Number AFATL-TR-84-15, 1984, 185 pp.

[19] Allemang, R.J., Brown, D.L., "A Correlation Coefficient for Modal Vector Analysis", Proceedings, International Modal Analysis Conference, pp.110-116, 1982.

[20] "Short Course Notes: Advanced Modal Analysis", University of Cincinnati, 1987.

[21] Van Der Auweraer, H., Snoeys, R., Leuridan, J.M., "A Global Frequency Domain Modal Parameter Estimation Technique for Mini-computers", to appear ASME, Journal of Vibration, Acoustics, Stress, and Reliability in Design.

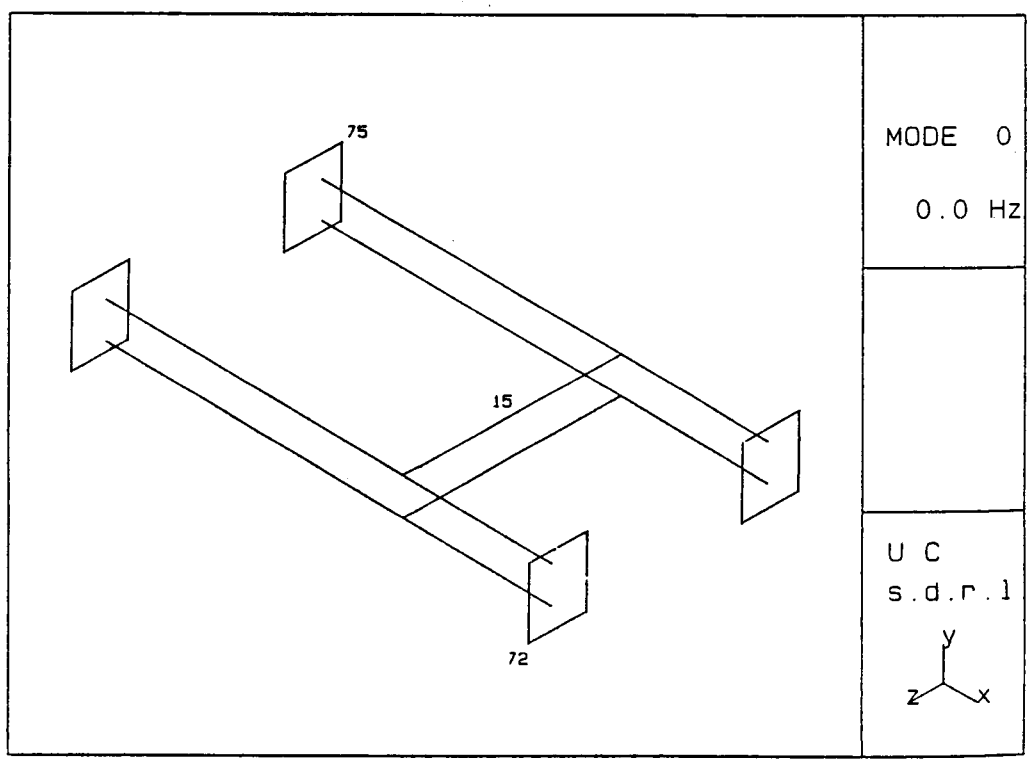

Figure 3. The H-frame structure with reference points shown

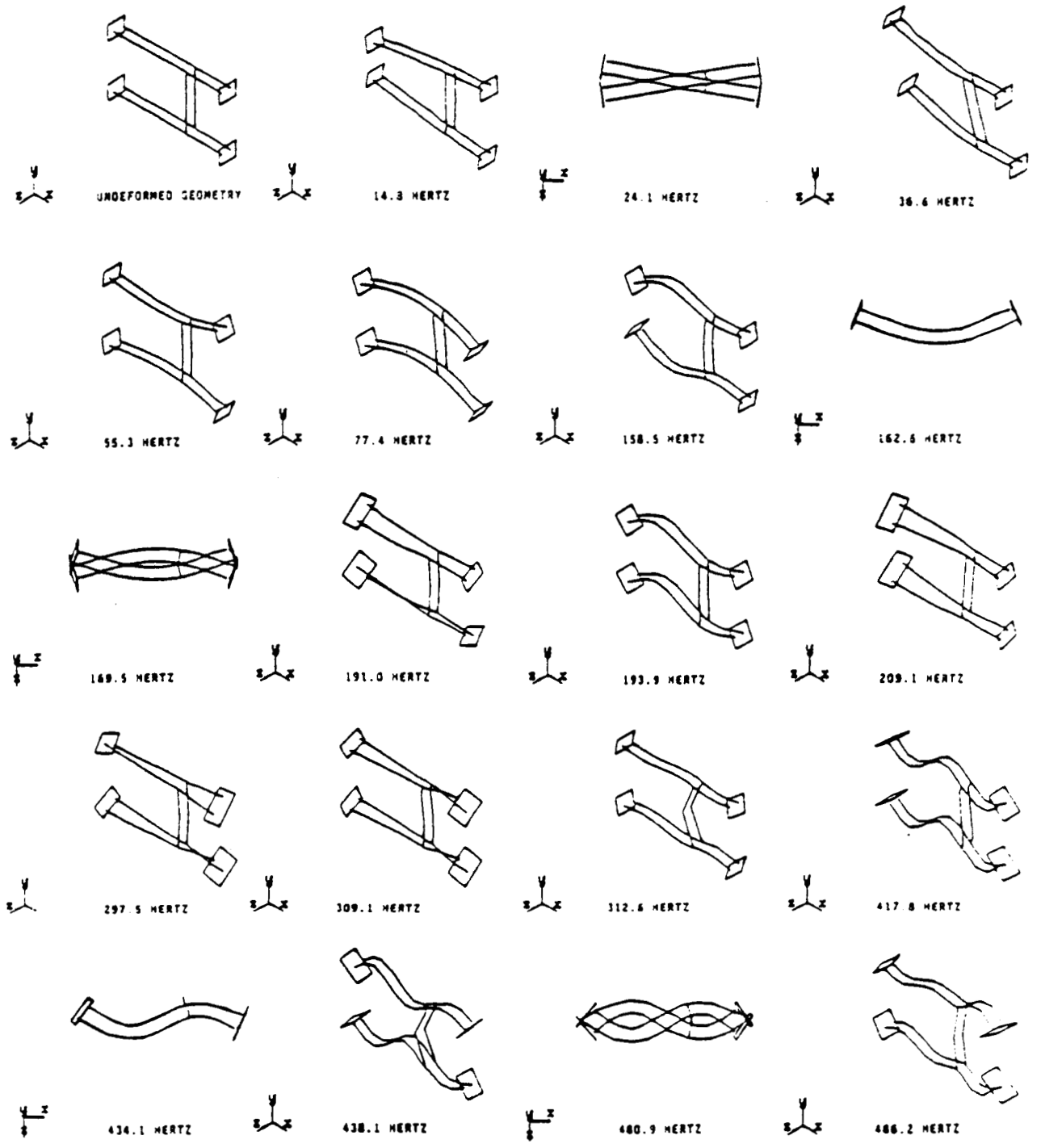

Figure 4. The original mode shapes of the H-frame structure

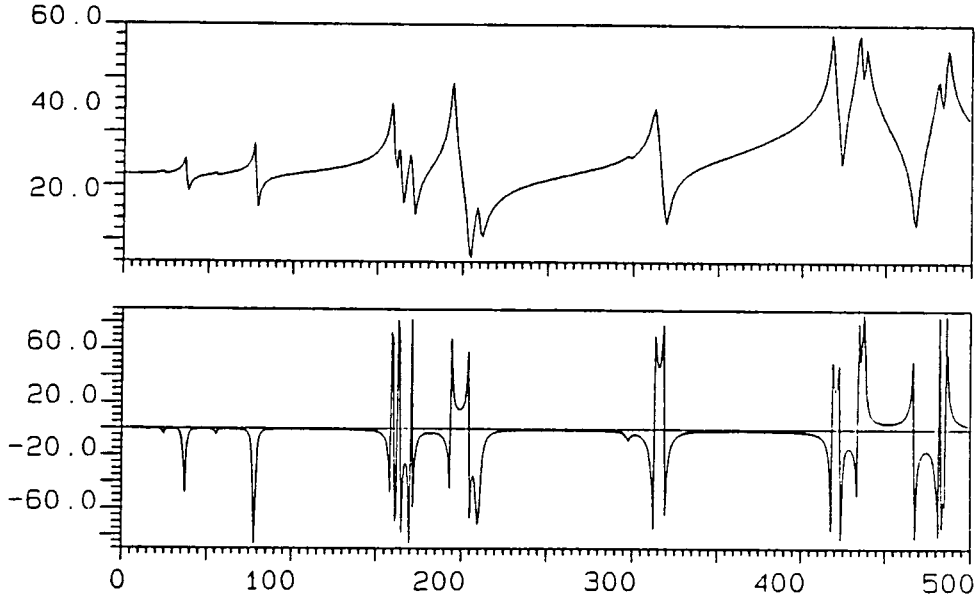

Figure 5. H-frame Driving Point Frequency Response Function

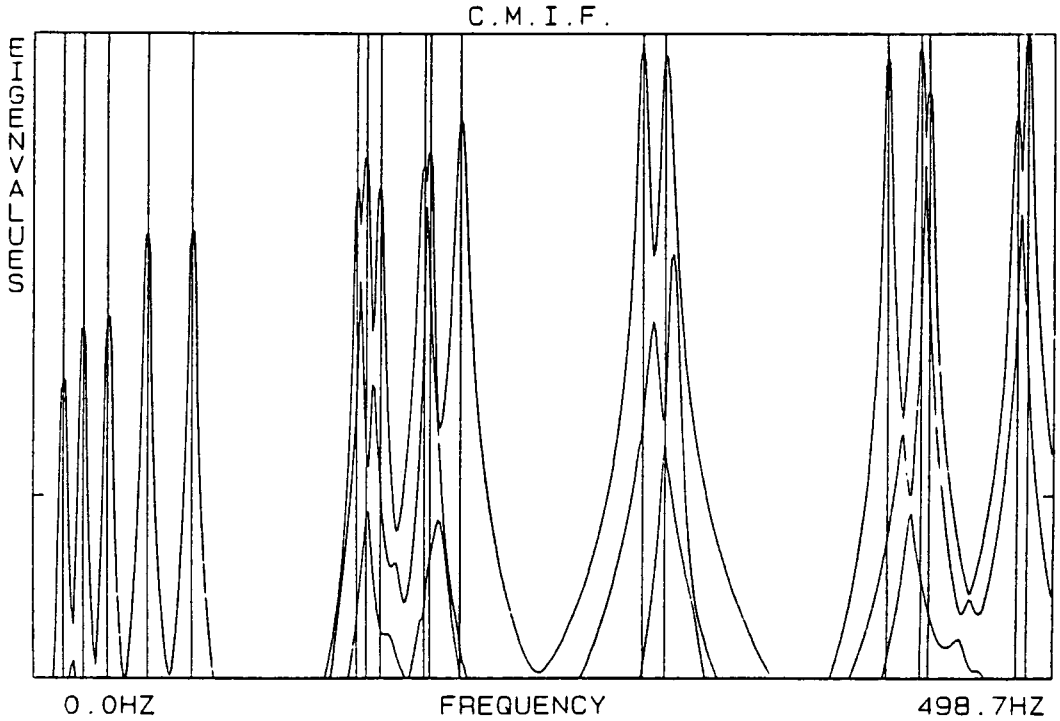

Figure 6. The CMIF plot of Case 1 data set, which showed mode 14 in second eigenvalue curve.

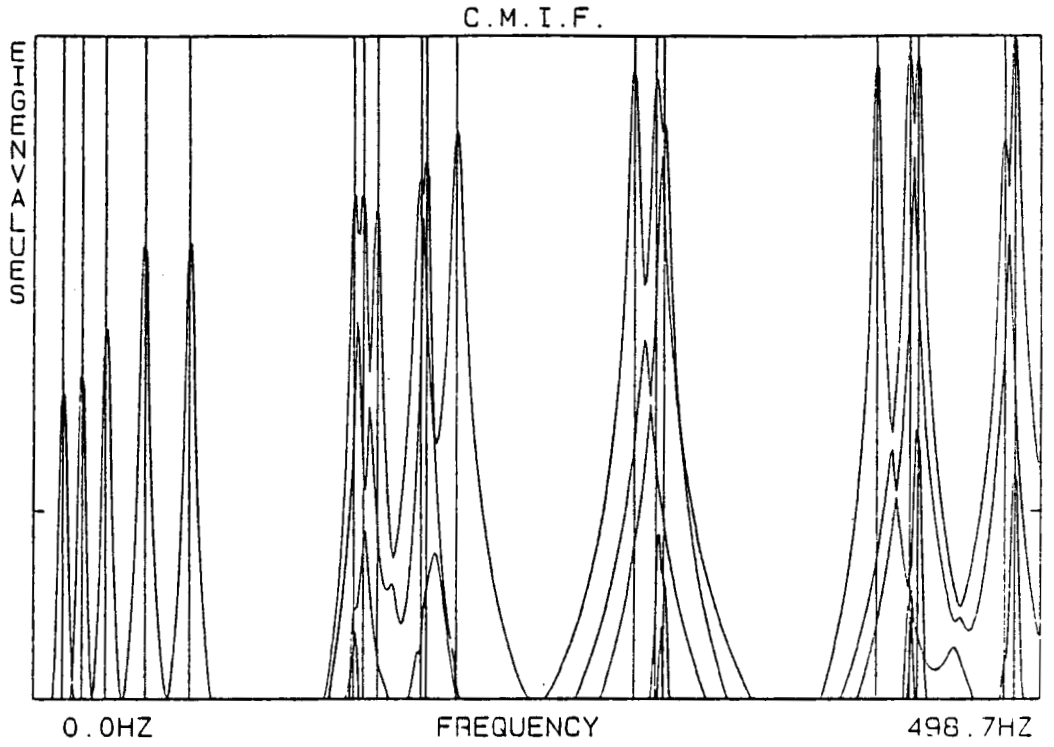

Figure 7. The CMIF plot of Case 2 data set, which showed 19 modes all exist in the largest eigenvalue curve.

Mode		Frequency/Damping Estimation Method				
		Data	PFD	MROP	MMEFRF	MMEFRF+
1	Freq. (Hz)	14.900	14.880	14.902	14.901	14.899
	Damp. (%)	5.148	5.149	5.149	5.147	5.152
2	Freq. (Hz)	24.087	24.094	24.086	24.087	24.087
	Damp. (%)	2.753	2.744	2.750	2.753	2.752
3	Freq. (Hz)	36.584	36.587	36.584	36.583	36.583
	Damp. (%)	1.984	1.965	1.981	1.984	1.984
4	Freq. (Hz)	55.294	55.291	55.294	55.293	55.293
	Damp. (%)	1.249	1.246	1.247	1.248	1.249
5	Freq. (Hz)	77.446	77.441	77.446	77.446	77.446
	Damp. (%)	0.901	0.992	0.900	0.901	0.901
6	Freq. (Hz)	158.539	158.527	158.541	158.540	158.541
	Damp. (%)	0.472	0.468	0.473	0.472	0.472
7	Freq. (Hz)	162.627	162.613	162.627	162.627	162.626
	Damp. (%)	0.611	0.611	0.611	0.612	0.612
8	Freq. (Hz)	169.477	169.492	169.477	169.477	169.477
	Damp. (%)	0.576	0.592	0.576	0.576	0.576
9	Freq. (Hz)	191.006	190.964	191.007	191.009	191.008
	Damp. (%)	0.793	0.755	0.793	0.795	0.795
10	Freq. (Hz)	193.900	193.896	193.900	193.901	193.896
	Damp. (%)	0.366	0.368	0.366	0.366	0.367
11	Freq. (Hz)	209.132	209.130	209.134	209.133	209.133
	Damp. (%)	0.759	0.743	0.759	0.761	0.761
12	Freq. (Hz)	297.551	297.523	297.551	297.550	297.549
	Damp. (%)	0.450	0.462	0.450	0.452	0.452
13	Freq. (Hz)	308.866	308.876	308.864	308.876	308.865
	Damp. (%)	0.539	0.561	0.539	0.542	0.538
14	Freq. (Hz)	312.401	312.529	312.402	312.106	312.402
	Damp. (%)	0.453	0.514	0.453	0.460	0.455
15	Freq. (Hz)	417.848	417.840	417.849	417.847	417.848
	Damp. (%)	0.198	0.205	0.198	0.198	0.198
16	Freq. (Hz)	434.071	434.044	434.071	434.066	434.076
	Damp. (%)	0.221	0.231	0.220	0.222	0.221
17	Freq. (Hz)	438.071	438.076	438.075	438.061	438.066
	Damp. (%)	0.211	0.212	0.212	0.213	0.213
18	Freq. (Hz)	480.966	480.961	480.968	480.971	480.977
	Damp. (%)	0.282	0.286	0.281	0.282	0.282
19	Freq. (Hz)	486.158	486.163	486.159	486.165	486.157
	Damp. (%)	0.209	0.213	0.209	0.212	0.212

Notes:

PFD	Polyreference Frequency Domain
MROP	Multiple-Reference Orthogonal Polynomial
MMEFRF	Multi-Mac Enhanced FRF
MMEFRF+	Multi-Mac Enhanced FRF with Case 2 data set.

TABLE 1. Comparison of estimated frequency and damping

Modal Assurance Criterion				
Mode	Mode Shape Estimation Method			
	PFD	MROP	MMEFRF	MMEFRF+
1	0.999	0.999	1.000	0.999
2	1.000	1.000	1.000	1.000
3	1.000	1.000	1.000	1.000
4	1.000	1.000	1.000	1.000
5	1.000	1.000	1.000	1.000
6	1.000	0.996	1.000	1.000
7	1.000	1.000	1.000	1.000
8	0.999	1.000	0.999	1.000
9	0.947	0.997	0.997	0.997
10	0.999	0.999	0.998	0.998
11	0.999	1.000	0.999	0.999
12	1.000	1.000	1.000	1.000
13	1.000	1.000	1.000	1.000
14	0.991	1.000	0.637	0.999
15	1.000	1.000	1.000	1.000
16	1.000	1.000	0.998	0.999
17	1.000	1.000	0.993	0.998
18	1.000	1.000	0.991	0.985
19	1.000	1.000	0.999	0.999

Notes:
PFD Polyreference Frequency Domain
MROP Multiple-Reference Orthogonal Polynomial
MMEFRF Multi-Mac Enhanced FRF
MMEFRF+ Multi-Mac Enhanced FRF with Case 2 data set.

TABLE 2. Comparison of estimated mode shapes by MAC